

## DESIGN OF A NANOTORI-METALLOFULLERENE LOGIC GATE

RICHARD K. F. LEE<sup>✉1</sup> and JAMES M. HILL<sup>2</sup>

(Received 7 March, 2013; accepted 22 May, 2015; first published online 25 August 2015)

### Abstract

We investigate the mechanics of a nano logic gate, comprising a metallofullerene which is located inside a square-shaped single-walled carbon nanotorus involving non-metallic, single-walled carbon nanotubes with perfect nanotoroidal corners. These are highly novel and speculative nanodevices whose construction, no doubt, involves many technical challenges. The energy for the system is obtained from the 6–12 Lennard-Jones potential with the continuous approximation. Our approach shows that there is not much difference between the energy when the metallofullerene is located in the tubes compared to when it is at the corners, and therefore the metallofullerene may be controlled by a small voltage. By applying two voltage inputs to produce external electric fields, one for the left–right motion and the other for the top–bottom motion, the metallofullerene can be moved to one of the four corners. Assuming that at the four corners there are charge detectors, the proposed device can be designed as a logic gate with different signals corresponding to particular gates.

2010 *Mathematics subject classification*: primary 97P60; secondary 82D80.

*Keywords and phrases*: carbon nanotubes, metallofullerenes, Lennard-Jones potential, nano-computational device, logic gate.

### 1. Introduction

In the past 35 years, the central processing unit (CPU) industry has followed Moore's prediction [35] that the complexity of integrated-circuit chips will double every two years simply by shrinking the size of transistors so that the processing speed increases, because the electric signals travel a shorter distance. Accordingly, the size of modern computers [35] is decreasing, resulting in improved speed and capacity and a reduction in energy and heat generation. However, physicists and engineers have already predicted that this trend will soon reach a barrier at 22 nm, since transistors will

<sup>1</sup>Tou Tsai Bui, Basement, Mercantile Industrial and Warehouse Building, 16–24 Ta Chuen Ping Street, Kwai Chung, New Territories, Hong Kong; e-mail: [Dr.RKF.Lee@gmail.com](mailto:Dr.RKF.Lee@gmail.com).

<sup>2</sup>School of Information Technology and Mathematical Sciences, University of South Australia, South Australia 5001, Australia; e-mail: [jim.hill@unisa.edu.au](mailto:jim.hill@unisa.edu.au).

© Australian Mathematical Society 2015, Serial-fee code 1446-1811/2015 \$16.00

TABLE 1. Basic logic gate.

| Input          |                | Output |       |       |       |
|----------------|----------------|--------|-------|-------|-------|
| I <sub>1</sub> | I <sub>2</sub> | AND    | OR    | NAND  | NOR   |
| TRUE           | TRUE           | TRUE   | TRUE  | FALSE | FALSE |
| TRUE           | FALSE          | FALSE  | TRUE  | TRUE  | FALSE |
| FALSE          | TRUE           | FALSE  | TRUE  | TRUE  | FALSE |
| FALSE          | FALSE          | FALSE  | FALSE | TRUE  | TRUE  |

become so small that the current fabrication technology and the basic physical laws pose severe limitations to further miniaturization [1, 15]. For example, the CPU industry is using 32 nm lithography techniques for the present smallest commercial transistors and it would be extremely difficult to fabricate transistors less than 22 nm using present techniques [3, 36]. Also, the heat released becomes a significant issue and the processing unit may be unstable, in which case the speed may not be improved. To overcome such difficulties, the CPU industry already manufactures several processors into a single unit, for example 2, 4, 6 or multicore chips [27]. To raise computational speed, parallel computing has been adopted, such as cloud computing or multithreads. Nanotechnology has brought about many revolutionary advanced materials, as many materials at the nanoscale display exceptional physical characteristics, for example mechanical and electronic properties, which [23], can be quite different from those at the macroscale. However, no progress will be made in this vital technology area until the realization of some specific devices is attempted. Accordingly, nanotechnological components may be one possible solution for future computer design. Since the first carbon nanomaterials were discovered, carbon nanotubes and fullerenes have been examined experimentally [28], theoretically [4, 25, 26, 31–33, 37] or computationally (molecular dynamics studies) [17, 24–26, 28, 33, 37] for possible use as memory devices.

A logic gate is a logical device that gives a result based on the input information. Table 1 shows the output result of the four basic logic gates: AND, OR, NAND and NOR. In the language of mathematical logic, an AND gate is that “the output is true if and only if both inputs are true”. In other words, the output for the AND gate will give the state TRUE information, when both inputs receive a state TRUE data, otherwise it will provide the state FALSE information. The other gates described in the language of mathematical logic are the following statements: “the output is true if and only if either input 1 or input 2 is true” for an OR gate; “the output is true if and only if the two inputs are not both true” for a NAND gate and “the output is true if and only if both inputs are false” for a NOR gate.

In this study, we propose a nanoscale logic gate comprising a metallofullerene situated inside a square-shaped single-walled carbon nanotorus comprising four non-metallic single-walled carbon nanotubes, with corners that are perfectly nanotoroidal as indicated in Figure 1. Both carbon fullerenes, carbon nanotubes and carbon nanotori

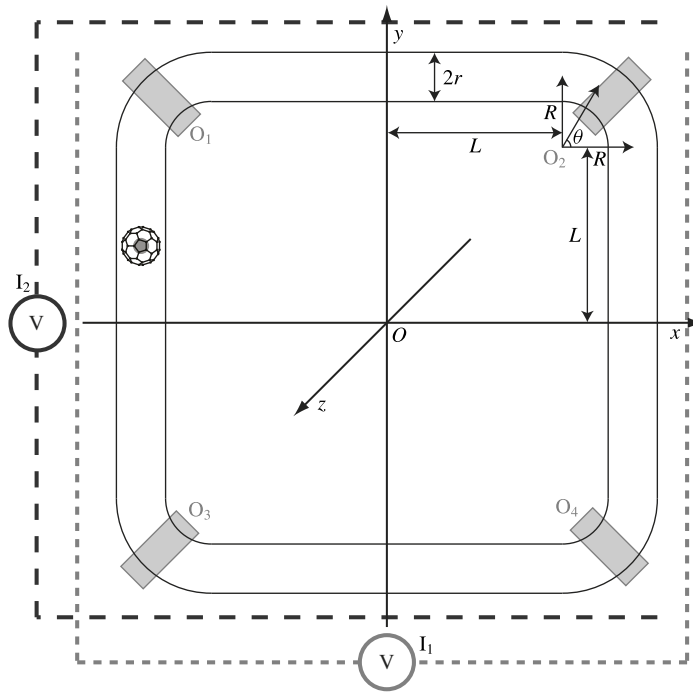


FIGURE 1. Proposed nano logic device.

are particular types of a carbon isomer. A  $C_{60}$  fullerene is a spherical carbon cage with a structure resembling that of a soccer ball with an empty centre [11], but which can contain an additional atom, such as  $F^-$ , Ne,  $Na^+$ ,  $Mg^{2+}$  or  $Al^{3+}$ , [6]. These are called endohedral fullerenes or endohedral metallofullerenes or simply metallofullerenes with an additional metal atom [2, 29], and we adopt the notation  $M@C_n$  where the symbol  $M$  is used to denote the additional metal atom inside the fullerene, and  $n$  indicates the total number of carbon atoms in the cage. The size of the endohedral fullerene is based on the number of carbon atoms  $n$  which ranges from 60 to 100. Iijima [18] discovered carbon nanotubes at NEC Corporation (Nippon Denki Kabushiki Gaisha) in 1991 which were conceptualized by a two-dimensional sheet rolled into a right circular seamless cylinder [12, 13, 22]. Nanotori are similar to doughnuts at the nanoscale and can be constructed from joined nanotubes [19–21, 34]. The square nanotorus considered here is assumed to comprise conventional nanotubes connected to four curved nanotubes of the same radius for the corners [7, 20]. Hilder and Hill [16] have investigated an atom or fullerene orbiting inside a closed carbon nanotorus, which is assumed to be perfectly toroidal.

Using applied mathematical modelling, we formulate the design rules to construct the proposed nano logical device consisting of a square-shaped nanotorus constructed from four carbon nanotubes joined together by corners which are a quarter of a perfect

torus, with a metallofullerene located inside it, as indicated in Figure 1. We assume that the carbon nanotubes are non-metallic to avoid any electrostatic interaction that may significantly complicate the analysis. In the next section, we introduce the method for the calculation of the potential function giving rise to the forces for this system. The potential energy of the 6–12 Lennard-Jones potential function is then introduced using the continuous approximation, which assumes an average constant atomic surface density. There is not much difference between the internal potential energy interactions of the metallofullerene at the corners of the nanotorus compared with in the tubes, and therefore we find it suitable for use as a logic gate. In Section 3, some numerical results are presented and discussed in relation to the design of logic gates. The paper concludes with some remarks in Section 4.

## 2. Methods

The proposed nano logic gate is shown in Figure 1, comprising a metallofullerene and a square-shaped carbon nanotorus involving a total of eight joined non-metallic carbon nanotubes (four straight and four curved). The total interaction energy  $E$  is the sum of the interaction energies for each non-bonded atomic pair  $\Phi(\rho_{ij})$ , that is,  $E = \sum_i \sum_j \Phi(\rho_{ij})$ , where  $\rho_{ij}$  is the distance between the non-bonded atoms  $i$  and  $j$ . However, since the proposed logic gate involves a large number of atoms, the total interaction energy is found from the continuous approximation which assumes that the total potential energy can be approximated by the double surface integral,

$$E = \eta_1 \eta_2 \int_{S_2} \int_{S_1} \Phi(\rho) dS_1 dS_2,$$

where  $\eta_1$  and  $\eta_2$  denote the mean atomic surface densities of each molecule, and  $\rho$  denotes the distance between the two typical surface elements  $dS_1$  and  $dS_2$ .

In this paper, the classical 6–12 Lennard-Jones potential is used to find the van der Waals interaction energy for the two non-bonded molecular structures. The 6–12 Lennard-Jones potential for two atoms at a distance  $\rho$  apart is given by

$$\Phi(\rho) = -(A/\rho^6) + (B/\rho^{12}),$$

where  $A$  and  $B$  denote the attractive and the repulsive constants, respectively [14], which can be rewritten as

$$\Phi(\rho) = 4\epsilon[-(\sigma/\rho)^6 + (\sigma/\rho)^{12}],$$

where  $\rho_0 = 2^{1/6}\sigma = (2B/A)^{1/6}$  is the equilibrium distance,  $\sigma$  is van der Waals diameter, and  $\epsilon = A^2/(4B)$  is the well depth [14]. The van der Waals diameter  $\sigma_{ab}$  and the well depth  $\epsilon_{ab}$  for two different materials, say materials  $a$  and  $b$ , are usually found from the empirical combining rules  $\epsilon_{ab} = (\epsilon_a \epsilon_b)^{1/2}$  and  $\sigma_{ab} = (\sigma_a + \sigma_b)/2$ , where the labels  $a$ ,  $b$  and  $ab$  refer to the interactions between  $a$  material,  $b$  material and  $ab$  materials, respectively [14]. The van der Waals interaction force  $F_{\text{vdW}}$  is found by differentiation of the total internal energy. Thus,  $F_{\text{vdW}} = -\nabla E$ , and the numerical values used for

TABLE 2. 6–12 Lennard-Jones constants and numerical values of constants.

|   |                                    |
|---|------------------------------------|
| Graphene–graphene [14]                          | $\rho_0 = 3.83 \text{ \AA}$        |
| Graphene–graphene [14]                          | $ \epsilon  = 2.39 \text{ meV}$    |
| C <sub>60</sub> –C <sub>60</sub> [14]           | $\rho_0 = 3.89 \text{ \AA}$        |
| C <sub>60</sub> –C <sub>60</sub> [14]           | $ \epsilon  = 2.86 \text{ meV}$    |
| C <sub>60</sub> –graphene [14]                  | $\rho_0 = 3.86 \text{ \AA}$        |
| C <sub>60</sub> –graphene [14]                  | $ \epsilon  = 2.62 \text{ meV}$    |
| K <sup>+</sup> –K <sup>+</sup> [5]              | $\rho_0 = 4.0010 \text{ \AA}$      |
| K <sup>+</sup> –K <sup>+</sup> [5]              | $ \epsilon  = 3.0352 \text{ meV}$  |
| Radius of (10, 10) [30]                         | $r = 6.766 \text{ \AA}$            |
| Radius of nanotorus                             | $R = 20 \text{ \AA}$               |
| Half length of nanotube                         | $L = 80 \text{ \AA}$               |
| Mean surface density of a single layer graphene | $\eta_g = 0.3812 \text{ \AA}^{-2}$ |
| Radius of C <sub>60</sub>                       | $b = 3.550 \text{ \AA}$            |
| Mean surface density of C <sub>60</sub>         | $\eta_f = 0.379 \text{ \AA}^{-2}$  |
| Radius of C <sub>80</sub>                       | $b = 4.200 \text{ \AA}$            |
| Mean surface density of C <sub>80</sub>         | $\eta_f = 0.370 \text{ \AA}^{-2}$  |
| Radius of C <sub>100</sub>                      | $b = 4.660 \text{ \AA}$            |
| Mean surface density of C <sub>100</sub>        | $\eta_f = 0.366 \text{ \AA}^{-2}$  |

the 6–12 Lennard-Jones constants for carbon nanostructures and potassium are as shown in Table 2. Overall, the given numerical values of the Lennard-Jones constants are in reasonable agreement with experimental results for both the high- and low-temperature phases [14]. Chen et al. [5] have proposed that potassium K can be ionized to K<sup>+</sup>, so that any induced charges on the single-walled carbon nanotube are uniformly distributed, and the Lennard-Jones potential can be used to calculate the internal energy of the system with a charged ion.

Cumings and Zettl [10] and Yu et al. [38] report that a multi-walled carbon nanotube system with an inner carbon nanotube oscillating inside an outer carbon nanotube exhibits almost zero friction between the inner and the outer tubes which hardly affects the motion, so that for the first approximation the frictional force may be ignored. As a result, there is virtually no frictional loss of energy involved in the motion of the metallofullerene, so that only the van der Waals interaction energy for the metallofullerene inside the square-shaped carbon nanotorus needs to be considered. Since the van der Waals' interactions are of short range, our basic model is as follows: if the metallofullerene is in the tube, we only calculate the interactions with the tube and the two adjacent corners; if the metallofullerene is at a corner, we only consider the interactions with the corner and the two adjacent tubes, as indicated in Figure 2 with solid black and dashed black lines. Since the square-shaped nanotorus is symmetrical, we only need to consider one tube and one corner, and the others are obtained by reflections. The nanotubes and the corners are considered to be perfect cylinders

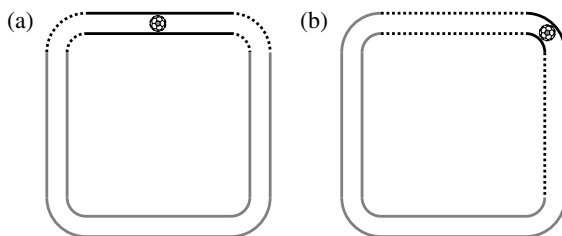


FIGURE 2. Interaction between metallofullerene and various parts for (a) metallofullerene inside nanotube and (b) metallofullerene inside corner.

and nanotori, respectively. Using the rectangular Cartesian coordinates  $(x, y, z)$  with origin  $O$  as indicated in Figure 3 and assuming that any atom for the top nanotube can be represented by  $(x, r \cos \phi + R, r \sin \phi)$ , any atom for the top right-hand corner can be represented by  $([R + r \cos \phi] \cos \theta, [R + r \cos \phi] \sin \theta, r \sin \phi)$ . For the other tubes and corners, it can be similarly represented by reflection of Figure 3(a). Also,  $(X, R, 0)$  and  $(R \cos \psi, R \sin \psi, 0)$  are the centres of the metallofullerene inside either the top nanotube or the top right corner, respectively, as shown in Figure 3, where  $r$  is the radius of the nanotube and the nanotorus;  $R$  is the radius of the nanotorus ring;  $\phi$  is the angle for the atoms located on the  $yz$ -plane for the top nanotube and  $\psi$  is the angle of the metallofullerene as measured from the top tube as shown in the Figure 3.

We assume that the entire motion of the metallofullerene is restricted to the two-dimensional  $xy$ -plane,  $Z = 0$ . However, even as a two-dimensional problem, the calculation is complex, and therefore, we reduce it to an one-dimensional problem by considering the two cases separately, namely, the metallofullerene located in the nanotube and that in the corner. The 6–12 Lennard-Jones potential vanishes at large distances, therefore the total interaction energy mainly comprises the interaction of the metallofullerene with the portion in which it is located and only with the joining parts. The total internal energy for the metallofullerene inside the nanotube  $E_T^{\text{vdW}}$  and inside the corner  $E_C^{\text{vdW}}$  is calculated from

$$E_T^{\text{vdW}} = E_{m-c1} + E_{m-t} + E_{m-c2} + E_{f-c1} + E_{f-t} + E_{f-c2}$$

and

$$E_C^{\text{vdW}} = E_{m-t1} + E_{m-c} + E_{m-t2} + E_{f-t1} + E_{f-c} + E_{f-t2},$$

where  $m, f, c1, c2, c, t1, t2$  and  $t$  indicate the metal, fullerene, left corner, right corner, inside corner, top nanotube, right nanotube and inside nanotube, respectively, as shown in Figure 3. The interaction for the corner  $c1$  is found from a reflection of the corner  $c2$  on the location  $x = -L$ , where  $L$  is the half-length of the nanotube, and the interaction for the nanotube  $t1$  is found from a reflection of the nanotube  $t2$  in the line  $x = y$ .

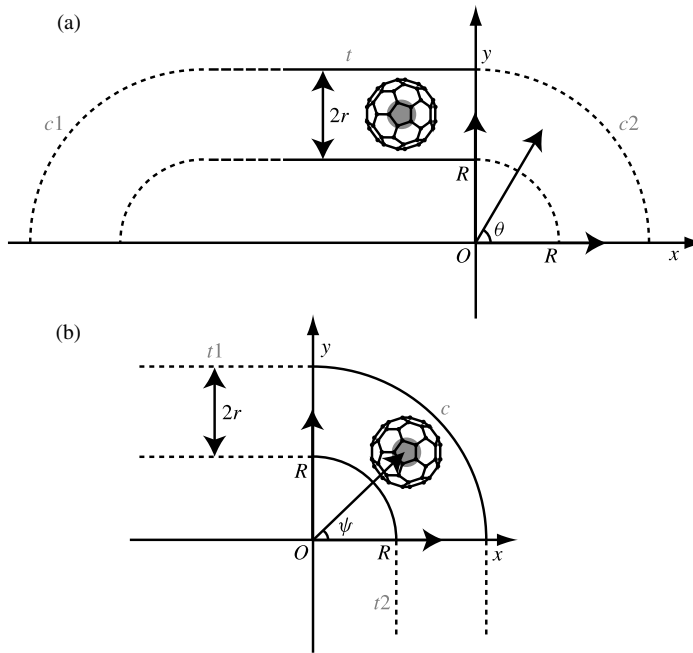


FIGURE 3. Interaction between metallofullerene and various parts for (a) metallofullerene inside nanotube and (b) metallofullerene inside corner.

In other words,

$$E_{i-c1}[\rho_{ct}(-X - 2L)] = E_{i-c2}[\rho_{ct}(X)]$$

and

$$E_{i-t1}[\rho_{tc}(\psi)] = E_{i-t2}[\rho_{tc}(\pi/2 - \psi)],$$

where the subscript for the energy  $i$  can be either  $m$  or  $f$  for the metal or fullerene, respectively, and the distances  $\rho_{ct}$  and  $\rho_{tc}$  denote the distance of the centre of the metallofullerene inside the corner to the atom of the nanotube and the distance of the centre of the metallofullerene inside the nanotube to the atom at the corner, respectively. Each energy has four distances to be considered: the centre of the metallofullerene inside the nanotube to an atom of the corner  $\rho_{tc}$  and to an atom of the nanotube  $\rho_t$ ; and the centre of the metallofullerene inside corner to an atom of the corner  $\rho_c$  and to an atom of the nanotube  $\rho_{ct}$ . These are, respectively,

$$\begin{aligned} \rho_t^2 &= r^2 + (X - x)^2, \\ \rho_{tc}^2 &= r^2 + X^2 - 2(R + r \cos \phi)[X \cos \theta + R \sin \theta - R], \\ \rho_c^2 &= 4R \sin^2 \beta (R + r \cos \phi) + r^2, \\ \rho_{ct}^2 &= r^2 + x^2 - 2xR \cos \psi + 2R(R + r \cos \phi)(1 - \sin \psi). \end{aligned} \tag{2.1}$$

The energy  $E_m(\rho)$  for the metal with one atom and the energy  $E_f(\rho)$  for the fullerene with one atom are as derived by Cox et al. [8, 9];

$$E_m(\rho) = -A/\rho^6 + B/\rho^{12}, \quad (2.2)$$

$$E_f(\rho) = \frac{\eta_f \pi b}{\rho} \left[ \frac{A}{2} \left\{ \frac{1}{(\rho+b)^4} - \frac{1}{(\rho-b)^4} \right\} - \frac{B}{5} \left\{ \frac{1}{(\rho+b)^{10}} - \frac{1}{(\rho-b)^{10}} \right\} \right], \quad (2.3)$$

where  $\eta_f$  is the mean surface density of fullerene and the numerical values of the 6–12 Lennard-Jones constants  $A$  and  $B$  are as in Table 2. The constants  $A$  and  $B$  for equations (2.2) and (2.3) have two different values arising from the metal ion with the nanotube or corner, and the fullerene with the nanotube or corner. Based on the equations (2.1)–(2.3), the total internal energies for the metallofullerene with the nanotube or the corner are given by

$$\begin{aligned} E_T^{\text{vdW}}(X) = r\eta_g \left[ \int_0^{\pi/2} \int_0^{2\pi} \{E_{m+f}(\rho_{tc}(-X-2L)) \times (R+r\cos\phi)\} d\phi d\theta \right. \\ \left. + 2\pi \int_{-2L}^0 E_{m+f}(\rho_t(X)) dx \right. \\ \left. + \int_0^{\pi/2} \int_0^{2\pi} \{E_{m+f}(\rho_{tc}(X))(R+r\cos\phi)\} d\phi d\theta \right], \quad (2.4) \end{aligned}$$

$$\begin{aligned} E_C^{\text{vdW}}(\psi) = r\eta_g \left[ \int_{-2L}^0 \int_0^{2\pi} E_{m+f}(\rho_{ct}(\psi)) d\phi dx + \int_{-2L}^0 \int_0^{2\pi} E_{m+f}(\rho_{ct}(\pi/2-\psi)) d\phi dx \right. \\ \left. + \int_0^{\pi/2} \int_0^{2\pi} \{E_{m+f}(\rho_c(\psi))(R+r\cos\phi)\} d\phi d\theta \right], \quad (2.5) \end{aligned}$$

where  $\rho_{tc}$ ,  $\rho_t$ ,  $\rho_{ct}$  and  $\rho_c$  are as in (2.1) and  $E_{m+f} = E_m + E_f$  and the numerical values of the constants  $R$ ,  $r$ ,  $b$ ,  $L$  and mean surface density of graphene  $\eta_g$  are as shown in Table 2.

### 3. Results and discussion

The potassium inside the fullerene is ionized to  $K^+$  which has a positive charge. In this system,  $K^+$  has only one positive charge and the fullerene and the nanotube are uniformly distributed and have no net charge, therefore the coulomb potential will not be considered. As a result, only the van der Waals potential for the  $K^+@C_{60}$  metallofullerene will be considered as the total energy.

Due to the complicated nature of the total energy equations (2.4) and (2.5), Figure 4 illustrates the numerical values of the total energies for the  $K^+@C_{60}$  metallofullerene in a (10, 10) square-shaped carbon nanotorus of half-length  $L = 80 \text{ \AA}$  and  $R = 20 \text{ \AA}$ . Figure 4(a) is the total interaction energy of a  $K^+@C_{60}$  metallofullerene inside a carbon nanotube with the left and the right corners and the nanotube. Figure 4(b) is the total interaction energy for a  $K^+@C_{60}$  metallofullerene inside the corner with the top and the right nanotube and the corner. The maximum and the minimum energy positions are located at the middle of the corner and the middle of the nanotube, respectively.

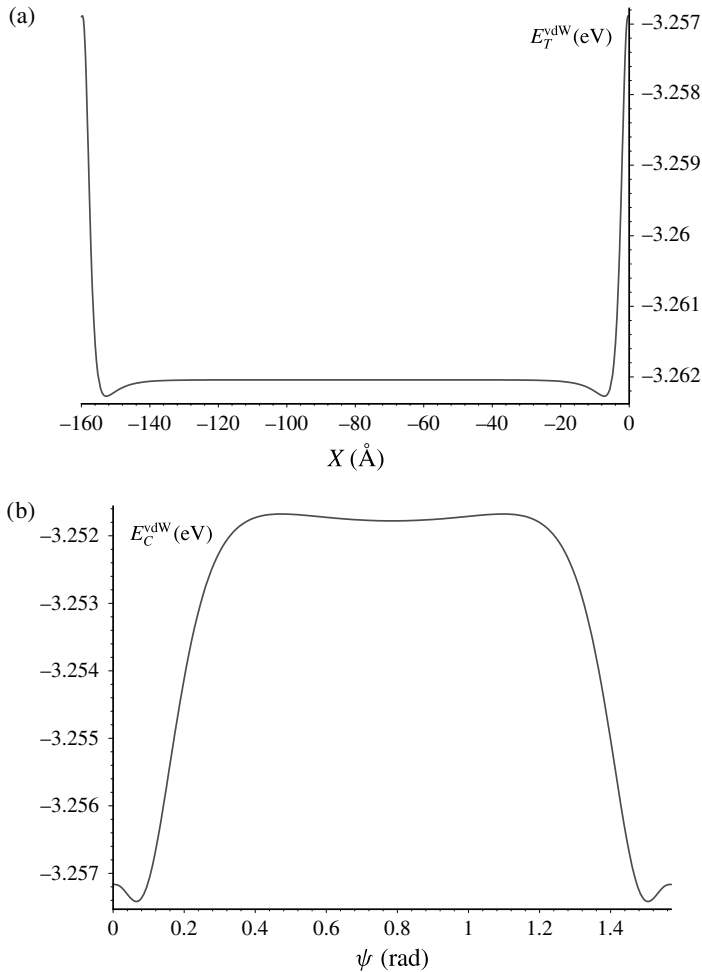


FIGURE 4. Internal energy for  $K^+@C_{60}$  in (10, 10) square-shaped carbon nanotorus of half-length  $L = 80 \text{ \AA}$  and  $R = 20 \text{ \AA}$ . (a)  $E_T^{vdW}$  for the metallofullerene in the nanotorus and (b)  $E_C^{vdW}$  for the metallofullerene in the corner.

The energy gap between the maximum energy from Figure 4(b) and the minimum energy from Figure 4(a) is around 0.01 eV, therefore the energy barrier is not sufficient to maintain the metallofullerene in the energy minimum location. However, based on the low energy barrier inside each corner, the metallofullerene may be controlled by using an external energy source.

This applied external force can be produced from an electrical field  $F_{\text{ext}} = qE$ , where  $q$  is the total charge of the metallofullerene and  $E$  is the magnitude of the external electrical field. When the ion in the metallofullerene has a double charge, the necessary external electrical field will be reduced to half of that for a single-charged

TABLE 3. Metallofullerene location and signal provided from releaser.

| $I_1$ | $I_2$ | Detector | AND | OR | NAND | NOR |
|-------|-------|----------|-----|----|------|-----|
| +     | +     | $O_4$    | +   | +  | -    | -   |
| +     | -     | $O_2$    | -   | +  | +    | -   |
| -     | +     | $O_3$    | -   | +  | +    | -   |
| -     | -     | $O_1$    | -   | -  | +    | +   |

ion. This logic gate is assumed to have two electrical field controllers for the two inputs,  $I_1$  and  $I_2$  as indicated in Figure 1. We also suppose that at each corner there is a charge detector to determine the metallofullerene location for the outputs,  $O_1$ ,  $O_2$ ,  $O_3$  and  $O_4$  as indicated by the grey boxes in Figure 1. The input will have a positive or a negative electrical field to represent input states TRUE or FALSE respectively, corresponding to Table 1. For the input  $I_1$ , a positive electrical field means that the electrical field is from left to right and a negative electrical field is in the opposite direction. For the input  $I_2$ , the positive electrical field is the direction from the top to the bottom and a negative electrical field is in the reverse direction. When both inputs  $I_1$  and  $I_2$  give a positive signal, the metallofullerene is going to the right bottom corner, so the detector  $O_4$  detects the charge from the metallofullerene. Table 3 shows the relationship between the input and the signal released from the releaser as a result of the detector determining the location of the metallofullerene. Figure 5 shows the nano logic gate design for AND, OR, NAND and NOR gates. For example, for the AND gate, if both inputs  $I_1$  and  $I_2$  have a positive signal, the detector  $O_4$  indicates that the metallofullerene is at the right bottom corner, and then the releaser provides a positive voltage. The releaser will generate a negative voltage for the metallofullerene at all the other detectors. As a result, it is an AND gate, because the releaser only provides a positive signal when both inputs give a positive signal. For the OR gate, the releaser will generate a negative voltage when the detector detects the metallofullerene at  $O_1$ . In the event of damage to the gate by the loss of charge from the metallofullerene, it will no longer function and there will be no output signal, because the charge detector will be unable to recognize the metallofullerene.

The proposed nano logic gate has three important dimensional parameters: the radius of the nanotube  $r$ , the radius of the nanotorus  $R$  and the length of the nanotube  $L$ . Following Chan et al. [4], since the metallofullerene is assumed to be located on the nanotube-axis with no offset, the radius of the nanotube  $r$  should be chosen to be as close as possible to 6.4 Å, 7 Å and 7.4 Å for the metallofullerenes  $M@C_{60}$ ,  $M@C_{80}$  and  $M@C_{100}$ , respectively. The radius of the nanotorus is a set value which is based on the size and the radius of nanotubes used to construct it [7]. A short length of nanotube improves the logic gate processing time (that is, the metallofullerene transit time). However, for short tubes the highly sensitive charge detectors may give a false signal due to the charged metallofullerene in a sensitive area; therefore the length of the nanotubes should be large enough for the sensitive areas of the four charge detectors

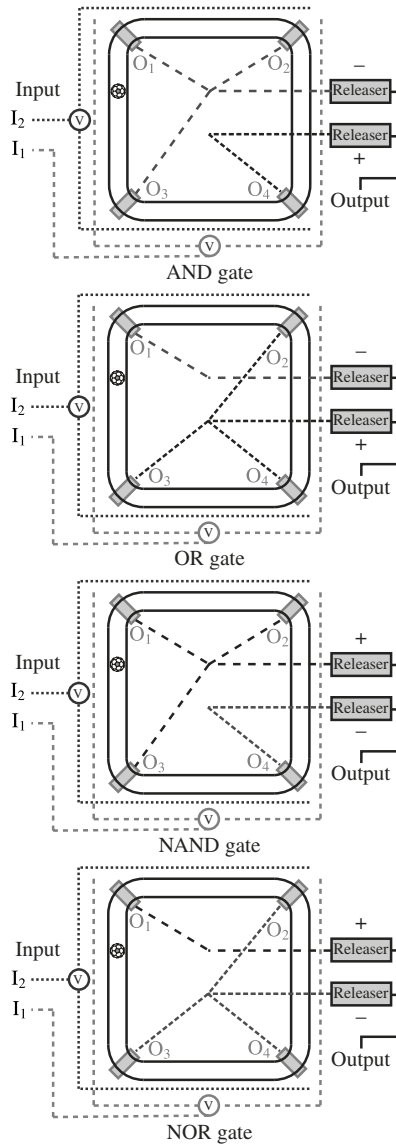


FIGURE 5. Design of nano logic gates.

not to overlap. Here we assume that the outputs are obtained from a device that is capable of measuring charge. The practical implementation of incorporating the inputs and reading such outputs will, no doubt, generate some considerable technical challenges. However, until some specific nanodevices are proposed for technical examination, very little progress will take place. Indeed, technical capability is constantly advancing to address such challenges.

In terms of the power consumption of the proposed nano logical device, we need to take into account the applied external force and the work done on the metallofullerene by the net force in moving from one stable state to another. In other words, we need to consider the work done in moving the metallofullerene from one corner to another through the input signals control. Depending upon the input and the initial location of the metallofullerene, there are four possible final locations: twenty five percent remain at the same corner, fifty percent move to the adjacent corners and twenty five percent move to the opposite corner, so that the work done takes on three values. If the metallofullerene remains in the same corner, the work done is zero. If the metallofullerene moves to an adjacent corner, the work done is given by

$$\begin{aligned}
 W &= \int_{\text{state 1}}^{\text{state 2}} F_{\text{net}} dZ \\
 &= F_{\text{ext}}(R\pi/4 + 2L + R\pi/4) + \int_{\pi/4}^{\pi/2} \left( -\frac{dE_C^{\text{vdW}}}{d\psi} \right) d\psi \\
 &\quad + \int_0^{-2L} \left( -\frac{dE_T^{\text{vdW}}}{dX} \right) dX + \int_{\pi/2}^{\pi/4} \left( -\frac{dE_C^{\text{vdW}}}{d\psi} \right) d\psi \\
 &= F_{\text{ext}}(R\pi/2 + 2L),
 \end{aligned}$$

where  $F_{\text{net}} = F_{\text{ext}} + F_{\text{vdW}}$ , and  $Z$  denotes the path of the metallofullerene moving from state 1 to state 2. Since the energy is an even function, the van der Waals term in the integral becomes zero, and for a constant external electrical field, the external force is also a constant. If the metallofullerene moves to the opposite corner, the work done is twice the work done  $W$ , because the path of the metallofullerene to the opposite corner is twice that of the metallofullerene moving to an adjacent corner. Consequently, the minimum and maximum possible values of work done are zero and  $2W$ , respectively, while on average, the work done is  $W$ .

#### 4. Summary

We propose a nano logic gate comprising a metallofullerene located inside a square-shaped, single-walled carbon nanotorus which is made up of four single-walled carbon nanotubes with four perfect nanotoroidal corners, all of which are assumed to be non-metallic to avoid electrostatic interactions. The metallofullerene is shown to have a low energy barrier, and therefore may be controlled by two small applied external electrical fields operating in two mutually perpendicular directions. The external electrical fields can be generated by the two voltage inputs,  $I_1$  and  $I_2$ , which control the left–right motion and the top–bottom motion, respectively. The location of the metallofullerene could then be determined by using a charge detector positioned at each corner. The left–right motion may be controlled by  $I_1$  while  $I_2$  controls the top–bottom motion. For the AND gate, the releaser provides a positive voltage for the detector  $O_4$  detecting the metallofullerene at the right bottom corner, when both the inputs  $I_1$  and  $I_2$  give positive signals, and the releaser provides a negative voltage for the metallofullerene

at the other detectors. For the other proposed gates, the releaser provides a specific voltage for the metallofullerene at the corresponding detector. For example, for the OR gate, the releaser provides a negative voltage when  $O_1$  detects the metallofullerene and a positive voltage for the metallofullerene at the other corner.

### Acknowledgement

The support of the Australian Research Council through the Discovery Project Scheme is gratefully acknowledged.

### References

- [1] W. Arden and K. H. Muller, "Physical and technological limits in optical and x-ray lithography", *Microelectron. Eng.* **6** (1987) 53–60; doi:10.1016/0167-9317(87)90016-5.
- [2] D. S. Bethune, R. D. Johnson, J. R. Salem, M. S. de Vries and C. S. Yannoni, "Atoms in carbon cages: the structure and properties of endohedral fullerenes", *Nature* **366** (1993) 123–128; doi:10.1038/366123a0.
- [3] T. M. Bloomstein, M. F. Marchant, S. Deneault, D. E. Hardy and M. Rothschild, "22 nm immersion interference lithography", *Opt. Express* **14** (2006) 6434–6443; doi:10.1364/OE.14.006434.
- [4] Y. Chan, R. K. F. Lee and J. M. Hill, "Metallofullerenes in composite carbon nanotubes as a nanocomputing memory device", *IEEE Trans. Nanotechnol.* **10** (2011) 947–952; doi:10.1109/TNANO.2010.2090170.
- [5] G. Chen, Y. Guo, N. Karasawa and W. A. Goddard III, "Electron–phonon interactions and superconductivity in  $K_3 C_{60}$ ", *Phys. Rev. B* **48** (1993) 13959; doi:10.1103/PhysRevB.48.13959.
- [6] J. Cioslowski and E. D. Fleischmann, "Endohedral complexes: atoms and ions inside the  $C_{60}$  cage", *J. Chem. Phys.* **94** (1991) 3730–3734; doi:10.1063/1.459744.
- [7] B. J. Cox and J. M. Hill, "New carbon molecules in the form of elbow-connected nanotori", *J. Phys. Chem. C* **111** (2007) 10855–10860; doi:10.1021/jp0721402.
- [8] B. J. Cox, N. Thamwattana and J. M. Hill, "Mechanics of atoms and fullerenes in single-walled carbon nanotubes. I. Acceptance and suction energies", *Proc. R. Soc. Lond. A* **463** (2007) 461–476; doi:10.1098/rspa.2006.1771.
- [9] B. J. Cox, N. Thamwattana and J. M. Hill, "Mechanics of atoms and fullerenes in single-walled carbon nanotubes. II. Oscillatory behaviour", *Proc. R. Soc. Lond. A* **463** (2007) 477–494; doi:10.1098/rspa.2006.1772.
- [10] J. Cumings and A. Zettl, "Low-friction nanoscale linear bearing realized from multiwall carbon nanotubes", *Science* **289** (2000) 602–604; doi:10.1126/science.289.5479.602.
- [11] W. I. F. David, R. M. Ibberson, J. C. Mattewman, K. Prassides, T. J. S. Dennis, J. P. Hare, H. W. Kroto, R. Taylor and D. R. M. Walton, "Crystal structure and bonding of ordered  $C_{60}$  buckminsterfullerene", *Nature* **353** (1991) 147–149; doi:10.1038/353147a0.
- [12] M. S. Dresselhaus, G. Dresselhaus and R. Saito, "Carbon fibers based on  $C_{60}$  and their symmetry", *Phys. Rev. B* **45** (1992) 6234–6242; doi:10.1103/PhysRevB.45.6234.
- [13] M. S. Dresselhaus, G. Dresselhaus and R. Saito, "Physics of carbon nanotubes", *Carbon* **33** (1995) 883–891; doi:10.1016/0008-6223(95)00017-8.
- [14] L. A. Girifalco, M. Hodak and R. S. Lee, "Carbon nanotubes buckyballs ropes and a universal graphitic potential", *Phys. Rev. B* **62** (2000) 13 104–13 110; doi:10.1103/PhysRevB.62.13104.
- [15] L. R. Harriott, "Limits of lithography", *Proc. IEEE* **89** (2001) 366–374; doi:10.1109/5.915379.
- [16] T. A. Hilder and J. M. Hill, "Orbiting atoms and  $C_{60}$  fullerenes in side carbon nanotori", *J. Appl. Phys.* **101** (2007) 064319; doi:10.1063/1.2511490.

- [17] H. J. Hwang, K. R. Byun, J. Y. Lee and J. W. Kang, "A nanoscale field effect data storage of bipolar endo-fullerenes shuttle device", *Curr. Appl. Phys.* **5** (2005) 609–614; doi:10.1016/j.cap.2004.08.005.
- [18] S. Iijima, "Helical microtubules of graphitic carbon", *Nature* **354** (1991) 56–58; doi:10.1038/354056a0.
- [19] S. Itoh and S. Ihara, "Toroidal form of carbon  $C_{360}$ ", *Phys. Rev. B* **47** (1993) 1703–1704; doi:10.1103/PhysRevB.47.1703.
- [20] S. Itoh and S. Ihara, "Toroidal forms of graphitic carbon. II. Elongated tori", *Phys. Rev. B* **48** (1993) 8323–8328; doi:10.1103/PhysRevB.48.8323.
- [21] S. Itoh and S. Ihara, "Isomers of the toroidal forms of graphitic carbon", *Phys. Rev. B* **49** (1994) 13 970–13 974; doi:10.1103/PhysRevB.49.13970.
- [22] R. A. Jishi, M. S. Dresselhaus and G. Dresselhaus, "Symmetry properties of chiral carbon nanotubes", *Phys. Rev. B* **47** (1993) 16 671–16 674; doi:10.1103/PhysRevB.47.16671.
- [23] P. V. Kamat and L. M. Liz-marzan, *Nanoscale materials* (Kluwer Academic Publishers, London, 2003).
- [24] J. W. Kang and H. J. Hwang, "A bucky shuttle three-terminal switching device: classical molecular dynamics study", *Physica E* **23** (2004) 36–44; doi:10.1016/j.physe.2003.11.271.
- [25] J. W. Kang and H. J. Hwang, "Carbon nanotube shuttle memory device", *Carbon* **42** (2004) 3018–3021; doi:10.1016/j.carbon.2004.06.014.
- [26] J. W. Kang and H. J. Hwang, "Schematics and simulations of nanomemory device based on nanopeapods", *Mater. Sci. Eng. C* **25** (2005) 843–847; doi:10.1016/j.msec.2005.06.038.
- [27] R. Kumar, V. Zyuban and D. M. Tullsen, "Interconnections in multi-core architectures: understanding mechanisms overheads and scaling", in: *Proceedings of the 32nd International Symposium on Computer Architecture* (IEEE, 2005) 408–419; doi:10.1109/ISCA.2005.34.
- [28] Y. K. Kwon, D. Tománek and S. Iijima, "Bucky shuttle memory device: synthetic approach and molecular dynamics simulations", *Phys. Rev. Lett.* **82** (1999) 1470–1473; doi:10.1103/PhysRevLett.82.1470.
- [29] K. Laasonen, W. Andreoni and M. Parrinello, "Structural and electronic properties of La-at- $C_{82}$ ", *Science* **258** (1992) 1916–1918; doi:10.1126/science.258.5090.1916.
- [30] R. K. F. Lee, B. J. Cox and J. M. Hill, "The geometric structure of single-walled nanotubes", *Nanoscale* **2** (2010) 859–872; doi:10.1039/B9NR00433E.
- [31] R. K. F. Lee and J. M. Hill, "Design of a two-state shuttle memory device", *CMC: Comput. Mater. Contin.* **20** (2010) 85–100; doi:10.3970/cmc.2010.020.085.
- [32] R. K. F. Lee and J. M. Hill, "Composite multiwalled carbon nanotubes as memory devices and logic gates", *J. Nanotechnol. Eng Med.* **3** (2012) 010902–010907; doi:10.1115/1.4006859.
- [33] J. Lee, H. Kim, S. J. Kahng, G. Kim, Y. W. Son, J. Ihm, H. Kato, Z. W. Wang, T. Okazaki, H. Shinohara and Y. Kuk, "Bandgap modulation of carbon nanotubes by encapsulated metallofullerenes", *Nature* **415** (2002) 1005–1008; doi:10.1038/4151005a.
- [34] V. Meunier, Ph. Lambin and A. A. Lucas, "Atomic and electronic structures of large and small carbon tori", *Phys. Rev. B* **57** (1998) 14 886–14 890; doi:10.1103/PhysRevB.57.14886.
- [35] G. E. Moore, "Progress in digital integrated electronics", *IEEE Tech. Digest* **21** (1975) 11–13; doi:10.1109/N-SSC.2006.4804410.
- [36] S. E. Thompson and S. Parthasarathy, "Moore's law: the future of Si microelectronics", *Mater. Today* **9** (2006) 20–25; doi:10.1016/S1369-7021(06)71539-5.
- [37] S. Xiao, D. R. Andersen and W. Yang, "Design and analysis of nanotube-based memory cells", *Nanoscale Res. Lett.* **3** (2008) 416–420; doi:10.1007/s11671-008-9167-8.
- [38] M. F. Yu, O. Lourie, M. J. Dyer, K. Moloni, T. F. Kelly and R. S. Ruoff, "Strength and breaking mechanism of multiwalled carbon nanotubes under tensile load", *Science* **287** (2000) 637–640; doi:10.1126/science.287.5453.637.